

AD-A102 751

NEW MEXICO STATE UNIV LAS CRUCES DEPT OF PHYSICS  
MODIFICATION OF SINGLE SCATTERING MODEL AGAUS.(U)  
MAY 81 E BURLBAW, A MILLER

F/6 20/6

DAAD07-80-M-4800

UNCLASSIFIED

ERADCOM/ASL-CR-81-0780-1 NL

1 OF 1  
AD A  
102-751

END

DATE  
FILMED

9-81

DTIC

ASL-CR-81-0780-1

**LEVEL**

AD

Reports Control Symbol  
OSD 1366

12

## MODIFICATION OF SINGLE SCATTERING MODEL AGAUS

MAY 1981

By

**EDWARD BURLBAW  
AUGUST MILLER**

Department of Physics  
New Mexico State University  
Las Cruces, New Mexico 88003

Under Contract DAAD0780-0

Contract Monitor: **RICHARD C. SHIRKEY**

Approved for public release; distribution unlimited



US Army Electronics Research and Development Command  
**ATMOSPHERIC SCIENCES LABORATORY**  
White Sands Missile Range, NM 88002

81 8 12 030

FILE COPY

AD A102251

SPOTIC  
ELECTED  
AUG 12 1981  
C

SECURITY CLASSIFICATION OF THIS PAGE (When Data Entered)

REPORT DOCUMENTATION PAGE		READ INSTRUCTIONS BEFORE COMPLETING FORM
1. REPORT NUMBER ASL-CR-81-0780-1	2. GOVT ACCESSION NO. AD-A102751	3. RECIPIENT'S CATALOG NUMBER
4. TITLE (and Subtitle) MODIFICATION OF SINGLE SCATTERING MODEL <u>AGAUS</u>		5. TYPE OF REPORT & PERIOD COVERED Contractor Report
7. AUTHOR(s) Edward Burlbaw and August Miller Contract Monitor: Richard C. Shirkey		8. CONTRACT OR GRANT NUMBER(s) DAAD07-80-M-4880 DAAD0780-0
9. PERFORMING ORGANIZATION NAME AND ADDRESS Department of Physics New Mexico State University Las Cruces, New Mexico 88003		10. PROGRAM ELEMENT, PROJECT, TASK AREA & WORK UNIT NUMBERS
11. CONTROLLING OFFICE NAME AND ADDRESS US Army Electronics Research and Development Command Adelphi, MD 20783		12. REPORT DATE May 1981
14. MONITORING AGENCY NAME & ADDRESS (if different from Controlling Office) US Army Atmospheric Sciences Laboratory White Sands Missile Range, New Mexico, 88002		13. NUMBER OF PAGES 28
		15. SECURITY CLASS. (of this report) UNCLASSIFIED
		15a. DECLASSIFICATION/DOWNGRADING SCHEDULE
16. DISTRIBUTION STATEMENT (of this Report)  Approved for public release; distribution unlimited		
17. DISTRIBUTION STATEMENT (of the abstract entered in Block 20, if different from Report)		
18. SUPPLEMENTARY NOTES  Contract Monitor: Richard C. Shirkey		
19. KEY WORDS (Continue on reverse side if necessary and identify by block number)  Mie theory Scattering Absorption Particles		
20. ABSTRACT (Continue on reverse side if necessary and identify by block number) An improved method for computation of phase functions has been implemented in computer code AGAUS to obtain more reliable results for large diameter particles under conditions of relatively high absorption. The new routine uses a partial backward recursion and the method of continued fractions. This represents an improvement over the forward recursion method. A brief outline of the later method is given for review and comparison. Results are presented which show that the new routine is reliable for Mie size parameters of at least 400 with an index of refraction as large as 5-5i.		

SECURITY CLASSIFICATION OF THIS PAGE(When Data Entered)



# CONTENTS

INTRODUCTION.....	5
MIE THEORY.....	6
SUBROUTINE MIEGX.....	12
VALIDATION OF THE CODE.....	18
LIST OF SYMBOLS USED IN MIEGX.....	22
MIEGX SIMPLIFIED FLOWCHART.....	25
RATIO OF CONSECUTIVE BESSEL FUNCTIONS - SIMPLIFIED FLOWCHART.....	26
NOTES ON FLOWCHART RATIO OF CONSECUTIVE BESSEL FUNCTION.....	27
REFERENCES.....	28

Accession For	
NTIS CR&I	<input checked="checked" type="checkbox"/>
DTIC TAB	<input type="checkbox"/>
Unannounced	<input type="checkbox"/>
Justification	
By	
Distribution/	
Availability Codes	
Avail and/or	
Dist	Special
A	

## INTRODUCTION

One of the most serious limitations of single scattering code AGAUS, as developed under previous contracts, was the inability of the internal Mie routine to provide reliable results for large diameter particles and situations involving relatively large absorption. These limitations have been reduced substantially through the replacement of the older forward recursion Mie routine by one using partial backward recursion and a method of continued fractions.

The new routine has been made operational on the HP computer system at the US Army Atmospheric Sciences Laboratory, White Sands Missile Range, NM, and has been coded to serve as a direct substitute for the earlier routine. This report has been written to serve primarily as documentation of the new routine. For the sake of completeness a brief review of the Mie theory has been included as well as symbolic definitions, flow charts for the new routine and a discussion of its reliability.

It should be noted that the new routine has been coded to have the same name (MIEGX) as the older Mie routine. This was done for ease of replacement by users who do not wish to revise other portions of AGAUS to reflect a change of name. The new routine can be easily distinguished from the older one by its use of complex arithmetic.

### MIE THEORY<sup>\*</sup>

Mie theory predicts the scattering by and the absorption in an isolated, discrete, homogeneous, isotropic sphere of diameter  $D$  with a known complex refractive index  $n = m - ik$  relative to the surrounding medium and illuminated by monochromatic radiant energy with wavelength  $\lambda$  in the surrounding medium. The theory is given in detail in standard texts and need not be repeated here. Instead, those elements of theory needed for an understanding of the numerical algorithms used are included.

All scattering properties of spheres are computed from  $m$  and  $k$ , and through the use of the induced electric and magnetic multipole moments of the sphere  $a_n$  and  $b_n$ , respectively. The moments are given by<sup>†</sup>

$$a_n = \frac{\psi'_n(n\alpha) \psi_n(\alpha) - n \psi_n(n\alpha) \psi'_n(\alpha)}{\psi'_n(n\alpha) \xi_n(\alpha) - n \psi_n(n\alpha) \xi'_n(\alpha)}, \quad (1)$$

and

$$b_n = \frac{n \psi'_n(n\alpha) \psi_n(\alpha) - \psi_n(n\alpha) \psi'_n(\alpha)}{n \psi'_n(n\alpha) \xi_n(\alpha) - \psi_n(n\alpha) \xi'_n(\alpha)}. \quad (2)$$

<sup>\*</sup> This section is partially based on material taken from ECOM report ECOM-5558 by R.B. Gomez, C. Petracca, C. Querfeld and G.B. Hoidale, March 1975, and the final report on Contract DAAD07-78-C-0063 by Miller et al., December 1978.

<sup>†</sup> Note that  $n$  is used as a subscript, an integer index and a complex index of refraction when it is not a subscript.

The prime denotes differentiation with respect to the argument. The  $\Psi_n(z)$  and  $\xi_n(z)$  functions are Ricatti-Bessel functions of the first and third kind, respectively, and are related to spherical Bessel functions  $j_n(z)$  and  $n_n(z)$  by

$$\Psi_n(z) = z j_n(z), \quad (3)$$

and

$$\xi_n(z) = z j_n'(z) - i z n_n(z) = \Psi_n'(z) + i \chi_n(z), \quad (4)$$

where

$$j_n(z) = \left(\frac{\pi}{2z}\right)^{\frac{1}{2}} J_{n+1/2}(z), \quad (5)$$

and

$$n_n(z) = \left(\frac{\pi}{2z}\right)^{\frac{1}{2}} N_{n+1/2}(z). \quad (6)$$

The function  $J_{n+1/2}(z)$  is the half integral order Bessel function; the function  $N_{n+1/2}(z)$  is the half integral order Neuman function.

The extinction cross section is computed from

$$C_{\text{ext}} = \frac{\lambda^2}{2\pi} \sum_{n=1}^{\infty} (2n+1) \operatorname{Re} (a_n + b_n), \quad (7)$$

and the scattering cross section from

$$C_{\text{sca}} = \frac{\lambda^2}{2\pi} \sum_{n=1}^{\infty} (2n+1) [|a_n|^2 + |b_n|^2]. \quad (8)$$

The various cross sections are the basic quantities used in scattering problems, but they are not the quantities usually computed directly from



Mie algorithms. Instead, it is more convenient to compute dimensionless efficiency factors  $Q_{\text{ext}}$  and  $Q_{\text{sca}}$ , which depend on  $n$ ,  $k$ , and  $\alpha$ , and which are multiplied by the geometrical sphere cross section to obtain the true cross section  $C_i = \pi r^2 Q_i$ . Thus,

$$Q_{\text{ext}} = \frac{2}{\alpha^2} \sum_{n=1}^{\infty} (2n+1) \operatorname{Re}(a_n + b_n), \quad (9)$$

and

$$Q_{\text{sca}} = \frac{2}{\alpha^2} \sum_{n=1}^{\infty} (2n+1) [|a_n|^2 + |b_n|^2]. \quad (10)$$

Although the cross sections account for the energy removed from the forward beam, they do not give any information about where the scattered photons go. This information is contained in scattering amplitudes and intensity factors which relate the flux density scattered through an angle  $\theta$  relative to the incident flux density. There are two amplitudes,  $S_1(\theta)$  and  $S_2(\theta)$ , and intensity factors  $i_1(\theta)$  and  $i_2(\theta)$ , which correspond to light respectively polarized perpendicular and parallel to the plane of scattering defined by the direction of incidence and the direction of scattering.

The intensity factors are related to the scattering amplitudes by

$$i_1(\theta) = |S_1(\theta)|^2, \quad (11)$$

$$i_2(\theta) = |S_2(\theta)|^2, \quad (12)$$

$$i_3(\theta) = \operatorname{Re}\{S_1 \cdot S_2^*\}, \quad \text{and} \quad (13)$$

$$i_4(\theta) = -\operatorname{Imag}\{S_1 \cdot S_2^*\}. \quad (14)$$

The amplitudes come from the multipole moments through

$$S_1(\theta) = \sum_{n=1}^{\infty} \frac{2n+1}{n(n+1)} [a_n \pi_n(\theta) + b_n \tau_n(\theta)], \quad (15)$$

and

$$S_2(\theta) = \sum_{n=1}^{\infty} \frac{2n+1}{n(n+1)} [b_n \pi_n(\theta) + a_n \tau_n(\theta)], \quad (16)$$

and angular factors  $\pi_n(\theta)$  and  $\tau_n(\theta)$  defined in terms of associated Legendre functions:

$$\pi_n(\theta) = P_n^1(\cos\theta)/\sin\theta, \quad (17)$$

$$\tau_n(\theta) = \frac{dP_n^1(\cos\theta)}{d\theta}. \quad (18)$$

The amplitudes have relative phase  $\delta = \arg S_1 - \arg S_2$ .

Alternative expressions frequently used are

$$\pi_n(\theta) = \frac{dP_n(\cos\theta)}{d(\cos\theta)}, \quad (19)$$

and

$$\pi_n(\theta) = \cos\theta \cdot \pi_n(\theta) - \sin^2\theta \cdot \frac{d\pi_n(\theta)}{d(\cos\theta)}, \quad (20)$$

where

$$P_n(\cos\theta) = \frac{1}{2^n n!} \frac{d^n}{d\cos^n\theta} (\cos^2\theta - 1)^n. \quad (21)$$

the single scattering albedo  $\tilde{\omega}_0$ , which gives the probability that the photon is scattered:

$$\tilde{\omega}_0 = \frac{1}{4\pi} \int_0^{2\pi} \int_{-1}^1 p(\theta) d\phi d\cos\theta = \frac{\lambda^2}{4\pi C_{\text{ext}}} \int_{-1}^1 [i_1(\theta) + i_2(\theta)] d\cos\theta \quad (26)$$

or

$$\tilde{\omega}_0 = C_{\text{sca}}/C_{\text{ext}} \quad (27)$$

For the special case of  $\theta = 180^\circ$ , backscatter, the efficiency is expressed by the radar cross section  $\sigma$ . The radar cross section may be defined as  $4\pi$  times the backscattered power per steradian divided by the incident power per unit area or

$$\sigma = 4\pi r^2 I(r, 180^\circ)/I_0 \quad (28)$$

This can be reduced by the relations

$$I(r, \theta) = \frac{I_0 \{i_1(\theta) + i_2(\theta)\}}{2k^2 r^2} \quad (29)$$

and

$$i_1(180^\circ) = i_2(180^\circ) = |s_1(180^\circ)|^2 \quad (30)$$

Thus

$$\sigma = \frac{4\pi}{k^2} |s_1(180^\circ)|^2 \quad (31)$$

and when divided by the geometrical cross section,  $G = \pi a^2$ ,

$$Q_{\text{radar}} = \frac{\sigma}{G} = \frac{4 |s_1(180^\circ)|^2}{a^2} \quad (32)$$

where  $\alpha = ka$ . Using

These functions satisfy the following recurrence relations:

$$\pi_n(\theta) = \cos\theta \frac{(2n-1)}{(n-1)} \pi_{n-1}(\theta) - \frac{n}{n-1} \pi_{n-2}(\theta), \quad (22)$$

and

$$\tau_n(\theta) = \cos\theta[\pi_n(\theta) - \pi_{n-2}(\theta)] - (2n-1)\sin^2\theta\pi_{n-1}(\theta) + \pi_{n-2}(\theta). \quad (23)$$

The scattering cross section measures the ability of a particle to scatter light, and it is to be expected that  $C_{sca}$  is obtained from an integral over the scattering intensity factors. Equation (8) follows from

$$C_{sca} = \frac{\lambda^2}{4\pi} \int_{-1}^1 (i_1(\theta) + i_2(\theta)) d\cos\theta. \quad (24)$$

Although the intensity factors themselves may be used in scattering calculations, they are primarily suited for computing flux densities, and it is frequently more convenient to measure and compute scattered light in terms of radiances. Radiances do not have the  $1/r^2$  dependence, and it is therefore unnecessary to know the distance from the scatterer to the detector if the detector field of view is small and is filled by the scattering cloud. The phase function  $p(\theta)$  gives a radiance  $I$  scattered into the  $\theta$  direction in terms of the radiance  $I_0$  incident on the particle.

The phase function is dimensionless and is defined here as

$$p(\theta) = \frac{\lambda^2}{2\pi C_{ext}} [i_1(\theta) + i_2(\theta)]. \quad (25)$$

The normalized phase function  $p(\theta)d\Omega/4\pi$  gives the probability of a photon being scattered through an angle  $\theta$  into an element of solid angle  $d\Omega = d\phi d\cos\theta$ . The integral of the normalized phase function is

$$-\pi_n(180^\circ) = \tau_n(180^\circ) = (-1)^n \cdot \frac{1}{2} n(n+1), \quad (33)$$

one obtains

$$-S_1(180^\circ) = S_2(180^\circ) = \sum_{n=1}^{\infty} (n + \frac{1}{2}) (-1)^n (a_n - b_n). \quad (34)$$

An alternate method of representing the phase functions is with series:

$$p(\theta) = \sum_{\ell=0}^{n-1} \tilde{a}_\ell P_\ell(\cos\theta), \quad (35)$$

where the Legendre expansion coefficients  $\tilde{a}_\ell$  are given by

$$\tilde{a}_\ell = \frac{(2\ell+1)}{2} \int_{-1}^1 p(\theta) P_\ell(\cos\theta) d(\cos\theta) \quad (36)$$

and  $P_\ell(\cos\theta)$  are the usual Legendre polynomials.

#### SUBROUTINE MIEGX

Subroutine MIEGX computes various efficiency factors, and intensity factors  $i_1$ ,  $i_2$ ,  $i_3$ , and  $i_4$  for each complex refractive index  $m$  and size parameter  $\alpha$  (or  $x$ ). The Ricatti-Bessel functions and their derivatives in Eqs. (1) and (2) are computed by the forward recursion method,

$$\xi_n(z) = \frac{2n-1}{z} \xi_{n-1}(z) - \xi_{n-2}(z), \quad (37)$$

where

$$\xi_n(z) = \psi_n(z) + i\chi_n(z), \text{ and } z \text{ is any complex quantity.}$$

The initial values used in forward recursion are

$$\psi_0(z) = \sin z,$$

$$\psi_1(z) = \frac{\sin z}{z} - \cos z,$$

$$\chi_0(z) = \cos z, \text{ and}$$

$$\chi_1 = \frac{\cos z}{z} + \sin z.$$

The angular functions  $\pi_n$  and  $\tau_n$  are also computed by forward recursions from Eqs. (22) and (23). The initial values used are  $\pi_0(\theta) = 0$ ,  $\pi_1(\theta) = 1$ ,  $\tau_0(\theta) = 0$ , and  $\tau_1(\theta) = \cos \theta$ .

For computational purposes it is more convenient to write Eqs. (1) and (2) in the following form<sup>+</sup>

$$a_n = \frac{\left[ \frac{A_n(n_i \alpha)}{n_i} + \frac{n}{\alpha} \right] \operatorname{Re}[\xi_n(\alpha)] - \operatorname{Re}[\xi_{n-1}(\alpha)]}{\left[ \frac{A_n(n_i \alpha)}{n_i} + \frac{n}{\alpha} \right] \xi_n(\alpha) - \xi_{n-1}(\alpha)} \quad (38)$$

$$b_n = \frac{[n_i A_n(n_i \alpha) + \frac{n}{\alpha}] \operatorname{Re}[\xi_n(\alpha)] - \operatorname{Re}[\xi_{n-1}(\alpha)]}{[n_i A_n(n_i \alpha) + \frac{n}{\alpha}] \xi_n(\alpha) - \xi_{n-1}(\alpha)}, \quad (39)$$

$$\text{where } A_n(n_i \alpha) = -\frac{n}{z} + \frac{J_{\nu-i}(n_i \alpha)}{J_\nu(n_i \alpha)} \quad (40)$$

and  $\nu = n + \frac{1}{2}$ . The symbol  $n_i$  is used here for the complex index of refraction to distinguish it from subscript  $n$ .

Methods utilizing either forward or backward recursion on the ratio have been applied to the problem and both methods have their own unique problems. Forward recursion methods are limited by the number of

<sup>+</sup>"Development of Programs for Computing Characteristics of Ultraviolet Radiation," IBM Corp., 1972, Technical Report for Contract No. NASS-21680 (NASA)

significant digits in the computer. Backward recursion methods must, of course, calculate  $A_N$  for some  $N$  larger than the  $n$  required for convergence of the Mie sums. Both methods usually require double precision arithmetic and have been shown to fail for cases involving large  $\alpha$  and/or a large imaginary part of the refractive index.

This subroutine uses the method of continued fractions<sup>†</sup> to calculate the ratio  $A_N$  independent of any previous value. The ratio is correct to the accuracy of the machine. The values of  $A_n$  for  $n < N$  are then calculated using the backward recursion formula

$$\frac{j_{n-2}(z)}{j_{n-1}(z)} = \frac{2n-1}{z} - \frac{j_n(z)}{j_{n-1}(z)} \quad (41)$$

If convergence of the Mie summations requires  $n > N$ , then  $A_{2N}$  is calculated, again independent of previous  $A_n$ 's, and backward recursion is used to calculate  $A_n$  for  $N+1 < n < 2N$ .

<sup>†</sup>This description is based, in part, on technical report ECOM 5509 (1973) AD767223 by W.J. Lentz. An article covering the same material can be found in Applied Optics 15, No. 3, 668 (1976).

A continued fraction may be written as

$$f = a_0 + \frac{b_1}{c_1 + \frac{b_2}{c_2 + \frac{b_3}{c_3 \dots}}} \quad (42)$$

or

$$f = a_0 + \frac{b_1}{c_1} + \frac{b_2}{c_2} + \frac{b_3}{c_3} + \dots \quad (43)$$

The  $n^{\text{th}}$  approximate convergent to the continued fraction representation of  $f$  is written as

$$f_n = a_0 + \frac{b_1}{c_1} + \dots + \frac{b_n}{c_n} \quad (44)$$

Continued fractions may be generated from a three-term recursion relation in a simple way:\*

$$\begin{aligned} \frac{J_{v-1}}{J_v} &= \frac{2v}{z} - \frac{J_{v+1}}{J_v} = \frac{2v}{z} - \frac{1}{\frac{2(v+1)}{z} - \frac{J_{v+2}}{J_{v+1}}} \\ &= \frac{2v}{z} - \frac{1}{\frac{2(v+1)}{z}} - \frac{1}{\frac{2(v+2)}{z}} - \dots \end{aligned} \quad (45)$$

So

$$\frac{J_{v-1}}{J_v} = 2vz^{-1} - \frac{1}{2(v+1)z^{-1}} - \frac{1}{2(v+2)z^{-1}} - \dots \quad (46)$$

\*For simplicity the argument  $z$  may be suppressed.



This form is one of a simple continued fraction which may be defined as

$$f(x) = a_1 + \frac{1}{a_2 + \frac{1}{a_3 + \frac{1}{a_4 + \dots \frac{1}{a_n + \dots}}} \quad (47)$$

where  $a_1 \neq 0$  and the  $a$ 's may be negative. Equation (47) may be written in the more convenient notation of

$$f(x) = [a_1, a_2, a_3, \dots]. \quad (48)$$

The  $n^{\text{th}}$  convergent is written in like manner:

$$f_n(x) = [a_1, a_2, a_3, \dots, a_n] \quad (49)$$

Lentz has shown that

$$f_n(x) = \frac{[a_1] \dots [a_{n-1}, \dots, a_1][a_n, \dots, a_1]}{[a_2] \dots [a_{n-1}, \dots, a_2][a_n, \dots, a_2]}. \quad (50)$$

The advantage of this method is that the calculation begins with the first term (rather than the end) of the fraction and is terminated when it is determined that

$$\left| \frac{[a_k, \dots, a_1]}{[a_k, \dots, a_2]} - 1 \right| < \epsilon. \quad (51)$$

The value of  $\epsilon$  depends on the accuracy needed or on the number of significant digits available on the computer used.

The ratio  $J_{v-1}/J_v$  can be written in a similar form with

$$a_n = (-1)^{n+1} 2(v+n+1)z^{-1}.$$

Subroutine MIEGX, as furnished, terminates the calculation of  $A_n$  with  $\epsilon = 10^{-6}$ . This could be decreased to increase speed at the loss of some accuracy. If the routine was converted to double precision it would be possible to set  $\epsilon$  to a much smaller value.

MIEGX then computes the preceding values of  $A_n$  by backward recursion and stores them to be used in the Mie summations of

$$\text{Re}[S_1(\theta)], \text{Im}[S_1(\theta)], \text{Re}[S_2(\theta)] \text{ and } \text{Im}[S_2(\theta)].$$

The sum is terminated when

$$|a_n|^2 + |b_n|^2 < \epsilon$$

and when the fractional change in the radar efficiency is also less than  $\epsilon$ , i.e., when

$$\left| \frac{Q_{\text{rad } n} - Q_{\text{rad } n-1}}{Q_{\text{rad}}} \right| < \epsilon .$$

This is more stringent than the first test alone and is a test on the phase functions as well.

MIEGX returns the following quantities as required by AGAUSX:

$Q_{\text{ext}}$ ,  $Q_{\text{sca}}$ ,  $Q_{\text{rad}}$ ,  $P(J)$ , PFNZRO, 01STAR, and 02STAR. The  $P(J)$  and PFNZRO as returned by MIEGX are average intensities and must be further normalized to become the actual phase functions (Eq. 25). 01STAR and 02STAR are the Legendre expansion coefficients  $\tilde{\omega}_1^*$  and  $\tilde{\omega}_2^*$ .

## VALIDATION OF THE CODE

Comparison runs of AGAUS using MIEGX with continued fractions and a previous version of MIEGX based on forward recursion were done in the region that the forward recursion routine is considered valid (see final report on Contract DAAD07-78-C-0063, December 1978). The comparison process was done mainly to verify that coding errors had been eliminated and that interfacing of the two was accomplished properly.

When one begins to test the limits of a code it is important to keep in mind the predictions of Mie theory. In the limit as  $\alpha \rightarrow \infty$ ,  $Q_{\text{ext}}$  is expected to converge to 2.0 for constant  $m$  and  $k$ . There may be fluctuations or ripples but these will be small for large  $\alpha$ . The absorption efficiency factor,  $Q_{\text{abs}}$ , is dependent on the imaginary part of the index of refraction.  $Q_{\text{abs}}$  will be small for the small imaginary part and approaches 1 for the totally absorbing sphere.  $Q_{\text{sca}}$  is the difference between  $Q_{\text{ext}}$  and  $Q_{\text{abs}}$  and therefore is bounded above by  $Q_{\text{ext}}$  for small imaginary part and equal to  $Q_{\text{ext}}$  for an all real index of refraction. For complex indices  $Q_{\text{sca}}$  will approach a value between  $Q_{\text{ext}} - Q_{\text{abs}}$  and  $Q_{\text{ext}}$ , i.e., between 1 and 2 as  $\alpha$  becomes large but at no time may  $Q_{\text{sca}}$  exceed  $Q_{\text{ext}}$ . The radar efficiency factor is expected to approach a limit between 0 and 1 as  $\alpha$  increases. The larger the value of  $k$  the smaller the asymptotic value of  $Q_{\text{radar}}$  is expected to be. Some oscillation is expected and it is possible that resonances can produce peak values much larger than the asymptotic value and minima near zero. Resonances may be more pronounced for  $k$  approximately 0. Values of  $Q_{\text{radar}}$  larger than 10 would probably be in error.

Table 1 shows the results of comparison calculations using MIEGX and DAMIE (a Mie routine written by J. V. Dave). The values of  $m$ ,  $k$ , and  $\alpha$  presented were chosen to show the agreement between the two codes as well as to point out the extended usefulness of MIEGX.  $Q_{\text{radar}}$  was included in the comparisons because it appears to be very sensitive to computational errors since it depends on the difference between  $a_n$  and  $b_n$ .  $Q_{\text{radar}}$  is also an indicator of the validity of the phase functions being itself  $p(180^\circ)$ .

For  $n = 1.2 - 0.01$  and  $\alpha = 10$  to  $400$ , there is exact agreement between MIEGX and DAMIE on the value of  $Q_{\text{ext}}$  and  $Q_{\text{sca}}$ . There is some variation between the two for  $Q_{\text{radar}}$ . Most interesting, though, is the large result for  $\alpha \approx 50$  obtained with both routines. This might be explained by resonance as mentioned previously.

The results obtained for  $n = 1.2 - 0.61$  show the failure of the DAMIE routine for large  $\alpha$ . As discussed above  $Q_{\text{sca}}$  must be less than  $Q_{\text{ext}}$ . A value of  $7.5$  ( $\alpha = 200$ ) is definite proof of failure. For  $\alpha = 100$  and larger,  $Q_{\text{radar}}$  has deviated dramatically from the value obtained with MIEGX. The presence of a slow downward trend in the MIEGX values of  $Q_{\text{ext}}$  and  $Q_{\text{sca}}$  as well the near constant value of  $Q_{\text{radar}}$  indicate that the routine is probably still valid for  $\alpha$  of  $400$ . The results for  $n = 1.2 - 1.21$  are presented to again display the extended usefulness of MIEGX with continued fractions.

Based on these results, as well as other test results not included in this report, MIEGX is likely to be reliable for  $\alpha$ 's of at least  $400$  with an index of refraction as large as  $5-5i$ . For the wide variety of test cases using MIEGX there has never been an obvious error in the calculation of  $Q_{\text{ext}}$  or  $Q_{\text{sca}}$ .

If the user has an application that requires unusual sizes and/or index of refraction combinations it is suggested that test runs be done that encompass the region of interest. Comparing the results to theory should provide an idea of the accuracy in that region.

Table 1. Comparison of MIEGX (with Continued Fractions) and DAMIE

Index of Refraction	$\alpha$	$Q_{\text{extinction}}$		$Q_{\text{scattering}}$		$Q_{\text{radar}}$	
		MIEGX	DAMIE	MIEGX	DAMIE	MIEGX	DAMIE
1.2 - 0.01	10	3.68513	3.68513	3.68513	3.68513	.039680	.039679
	50	1.98649	1.98469	1.98649	1.98649	6.77499	6.77482
	100	1.99914	1.99914	1.99914	1.99914	.732798	.732791
	200	2.11768	2.11768	2.11768	2.11768	1.98705	1.98709
	300	2.02145	2.02145	2.02145	2.02145	.370321	.370399
	400	2.02705	2.02705	2.02705	2.02705	.893983	.893958
1.2 - 0.61	10	2.30026	2.30026	1.18524	1.18524	.075242	.075242
	50	2.12796	2.12796	1.20466	1.20466	.076935	.076935
	100	2.08388	2.03221	1.19399	1.20682	.076926	.003914
	200	2.05425	2.15197	1.18318	7.52386	.076926	26.4102
	300	2.04188	2.09972	1.17762	10.4743	.076924	67.5684
	400	2.03480	1.99701	1.17409	11.7734	.076925	.076189
1.2 - 1.21	10	2.45449	2.45449	1.45406	1.45406	.240903	.240903
	50	2.16159	2.161595	1.38346	1.38346	.235709	.235707
	100	2.10076	2.07393	1.35930	1.64276	.235682	10.7535
	200	2.06264	2.06602	1.34127	4.18491	.235676	63.9834
	300	2.04744	2.02119	1.33318	4.33033	.235673	13.8803
	400	2.03895	2.04184	1.32836	4.57723	.235675	.231767

# List of Symbols used in MIEGX

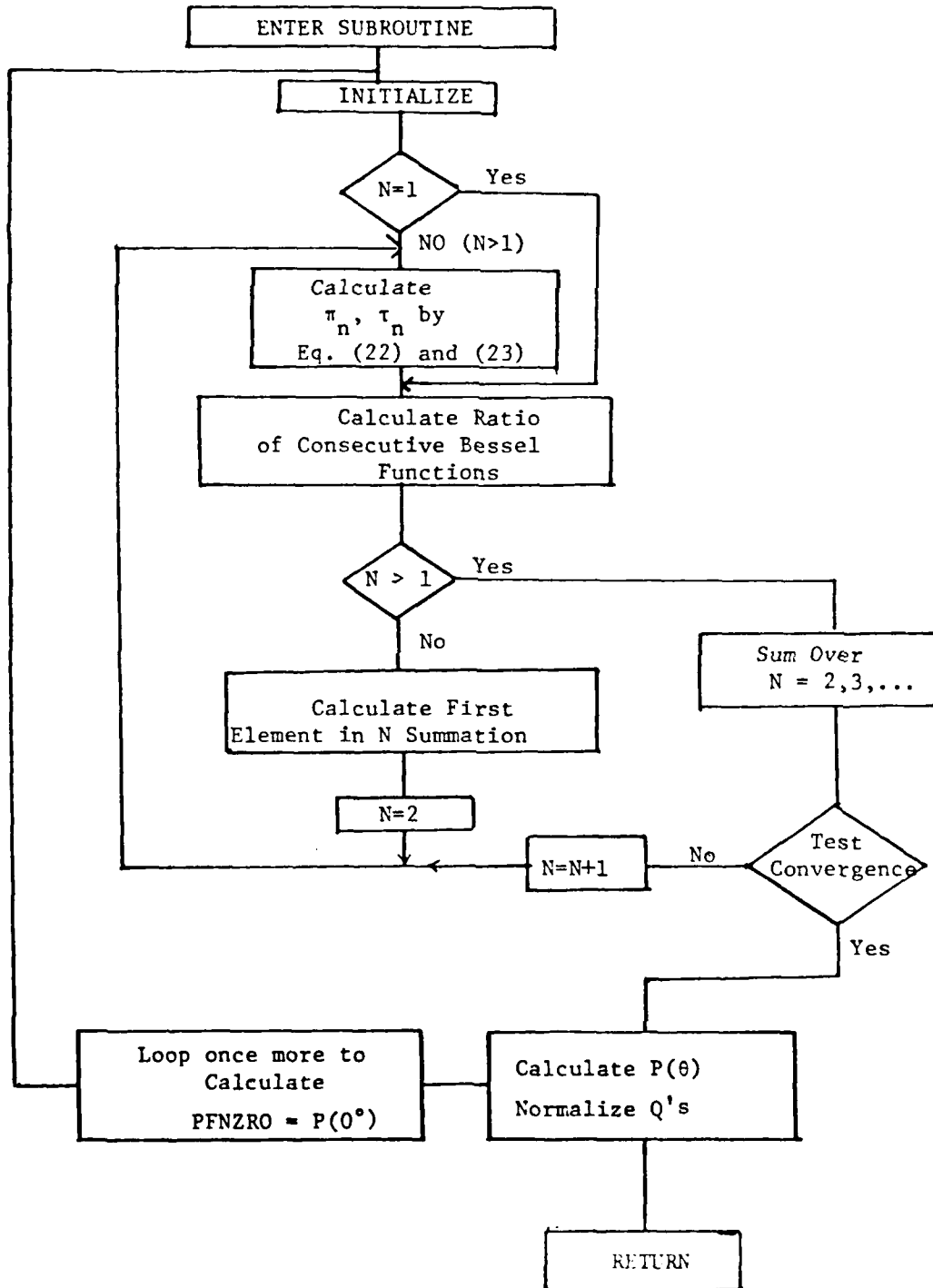
SYMBOL	Explanation or Definition
A(J)	$A_n$ (Eq. 40) the array
ACAPN	$A_n$ for the current n of the Mie sum
ALPHA,X	Mie size parameter, $\alpha = X = 2\pi r/\lambda$
ALPHAD	Double precision ALPHA
C(J),CJ	The array of cosines of the scattering angles; there are 'IT' elements in the array, the Jth element, respectively.
CAY,CAYD	The ratio of the imaginary part to the real part of adjusted refractive index, double precision CAY, respectively.
CAYE	The true imaginary part of adjusted refractive index
ELTRMX(1,J)	Within n loop: $= \text{Re}[S_1(\theta)]$ ; after n loop: $= i_2 = S_2(\theta) \cdot S_2^*(\theta)$
ELTRMX(2,J)	Within n loop: $= \text{Im}[S_1(\theta)]$ ; after n loop: $= i_1 = S_1(\theta) \cdot S_1^*(\theta)$
ELTRMX(3,J)	Within n loop: $= \text{Re}[S_2(\theta)]$ ; after n loop: $= i_3 = \text{Re}[S_1(\theta) \cdot S_2^*(\theta)]$
ELTRMX(4,J)	Within n loop: $= \text{Im}[S_2(\theta)]$ ; after n loop: $= (-i_4) = \text{Im}[S_1(\theta) S_2^*(\theta)]$
EM,EMD	The real part of adjusted refractive index, double precision EM, respectively.
EN,ENL1	Floating point representation of N, N-1, respectively.
FNA,FNAP,FNAPP	$= a_n, a_{n-1}, a_{n-2}$ , respectively.
FNB,FNBP,FNBPP	$= b_n, b_{n-1}, b_{n-2}$ , respectively.
N	Index in Mie sum
NDELTA	The smaller of NDIM and NMX, later used as increment of N for calculation of $A_n$
NDIM	The dimension of A array
NMX	$= X*(m+k)+9$ an approximation to the maximum N needed
NMIN	$= \text{NMX}+1-\text{NDELTA}$

<u>SYMBOL</u>	<u>Explanation or Definition</u>
01STAR,01STRD	$= \bar{\omega}_1^*$ ; first order coefficient for Legendre expansion of the average intensity $P(J)$ , double precision 01STAR respectively
02STAR,02STRD	$= \bar{\omega}_2^*$
P(J)	$= (i_1 + i_2)/2$ , the average intensity at angles, $\arccos(C(J))$ . 'IT' elements in array
PFNZRO	= the average intensity at $0^\circ$
PI(1,J),PI(2,J) PI(3,J)	$= \pi_{n-2}(\theta), \pi_{n-1}(\theta), \pi_{n-3}(\theta)$ (Eq. 22)
PI1J,PI2J,PI3J	The Jth element of PI(1,J), PI(2,J) and PI(3,J), respectively
QEXT	Unnormalized efficiency factors
QRD	Double precision backscatter efficiency factor
QRT	$= \text{SUMRR}^2 + \text{SUMRI}^2$ present value of unnormalized backscatter cross section
QRTL2	Previous value of QRT
QTR	$=  QRT - QRTL1 /QRT$ , ratio of change in QRT to present value - used as part of exit criterion
QSCAT	The unnormalized scattering cross section
QSD	Double precision scattering efficiency factor
QTD	Double precision extinction efficiency factor
RF	$= \text{EM} - i\text{CAYE}$ , complex refractive index
RRF	$= 1/\text{RF}$
RRFX	$= 1/(X*\text{RF})$
RX	$= 1/X$
SGR	The backscattering (radar) efficiency factor
SGS	The scattering efficiency factor
SGT	The extinction efficiency factor
SUMRR	$= \sum_{n=1}^N (-1)^n (2n+1) \text{Re}[a_n - b_n]$

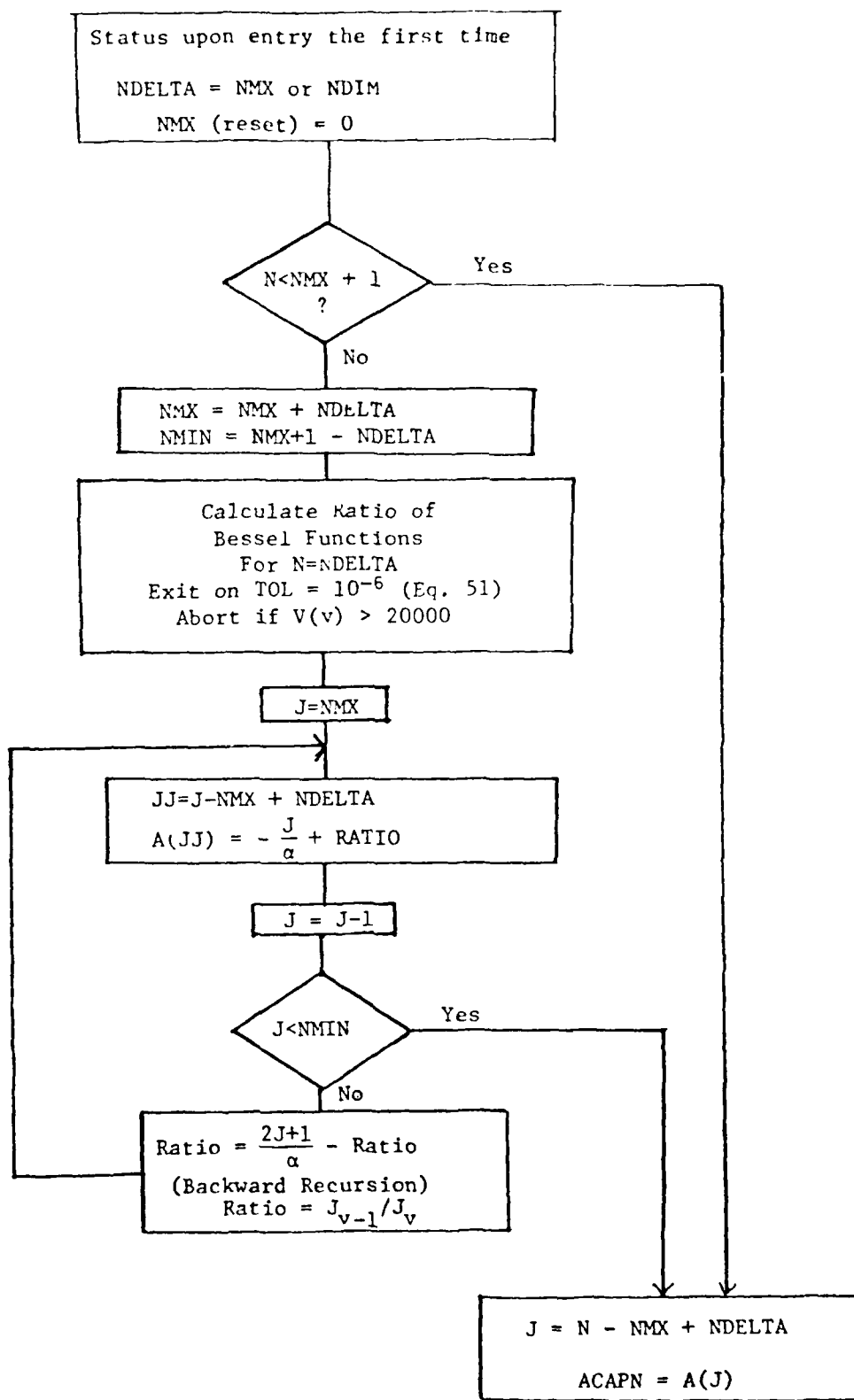


<u>SYMBOL</u>	<u>Explanation or Definition</u>
SUMRI	$= \sum_{n=1}^N (-1)^n (2n+1) \operatorname{Im}[a_n - b_n]$
T(5)	Temporary storage variables (real)
TA(1),TA(2)	Real and imaginary parts of WFN(1), respectively
TA(3),TA(4)	Real and imaginary parts of WFN(2), respectively
TAU(1,J),TAU(2,J), TAU(3,J)	$= \tau_{n-2}(\theta), \tau_{n-1}(\theta), \tau_n(\theta)$ respectively
TAU2J,TAU2J,TAU3J	The Jth element of TAU(1,J), TAU(2,J), and TAU(3,J), resp.
TB(1),TB(2)	Real and imaginary part of FNA, respectively
TC(1),TC(2)	Real and imaginary part of FNB, respectively
TD(1),TD(2)	Real and imaginary parts of FNAP, respectively
TE(1),TE(2)	Real and imaginary part of FNBP, respectively
TF(1),TF(2)	Real and imaginary parts of FNAPP, respectively
TG(1),TG(2)	Real and imaginary parts of FNBPP, respectively
TC1	$= (A_n/n_1) + (n/x)$
TC2	$= (A_n \cdot n_1) + (n/x)$
TOL	$= 1.E-06$ exit tolerance for Mie sum
V	$= NMX + 3/2$
WM1	$= \xi_{n-2}(x)$
WFN(1)	$= \xi_{n-1}(x)$
WFN(2)	$= \xi_n = \frac{2n-1}{x} \xi_{n-1}(x) - \xi_{n-2}(x)$
X,ALPHA	$= 2\pi r/\lambda$
Y	$= X*RF$
ZAN,ZANP ZDEN,ZNUM	Temporary complex valued variables in continued fractions calculation of $A_n$

# MIEGX - Simplified Flowchart



# RATIO OF CONSECUTIVE BESSEL FUNCTIONS - Simplified Flow Chart



#### NOTES ON FLOWCHART RATIO OF CONSECUTIVE BESSEL FUNCTION

What seems to be a confusing use of variables within the calculation loop; namely NMX, NMIN, NDELTA, JJ and J, is necessary because the way the A array is used. The first time through, the ratio  $J_{v-1}/J_v$  and  $A_N$  is calculated for the largest value of N that might be needed or is allowed by array size. The ratio is calculated using the continued fractions routine and the preceding  $A_n$ 's are calculated using backward recursion. If the Mie sum does not converge before it uses all the calculated  $A_n$  then it becomes necessary to calculate the next  $A_n$  values. If so the ratio and  $A_N$  are recalculated for a new largest N (this time twice the original N) and the previous N values of  $A_n$  replace the former array elements, i.e., the A array now contains  $A_{N+1}, \dots, A_{2N}$ . When this is done the Mie sum continues. This calculation and replacement of the A array continues until the Mie sum converges.

## References

1. A. Miller, G.H. Goedecke, R.C. Shirkey, Y.K. Behl, Studies on the Development of Algorithms for the Prediction of Time-Dependent Optical Properties of Aerosols, NMSU Dept. of Physics, December 1978; Final Report for Contract DAAD07-78-C-0063.
2. H. C. Van de Hulst, Light Scattering by Small Particles, John Wiley & Sons, Inc., New York, 1957.
3. W. J. Lentz, A New Method of Computing Spherical Bessel Functions of Complex Argument with Tables, ECOM-5509, 1973.
4. W. J. Lentz, Generating Bessel functions in Mie scattering calculations using continued fractions, Applied Optics 15, No. 3, 668 (1976).
5. J. V. Dave, Development of Programs for Computing Characteristics of Ultraviolet Radiation, IBM Corp., 1972, Technical Report for Contract No. NAS5-21680 (NASA).

DATE  
FILMED  
-18